Emission of low-energy charged particles following negative-pion capture from rest

F. W. Schlepütz,* J. C. Comiso, T. C. Meyer,† and K. O. H. Ziock

Physics Department, University of Virginia, Charlottesville, Virginia 22901

(Received 25 July 1978)

We have measured the inclusive production spectra of protons, deuterons and α particles following negative pion capture from rest in carbon, calcium, indium, and bismuth from low energies up to 55 MeV for protons and deuterons, and 30 MeV for α particles. The proton and deuteron spectra separate into contributions from direct processes and from evaporation. The integrated production rates are in agreement with previous results. The data are compared with various theoretical models.

$$\left[\begin{array}{c} \text{NUCLEAR REACTION } {}^{12}\text{C, } {}^{40}\text{Ca, } {}^{115}\text{In, } {}^{209}\text{Bi, measured spectra of } p,\ d,\ \alpha \text{ fol-} \\ \text{lowing } \pi^- \text{ absorption.} \end{array}\right]$$

I. INTRODUCTION

The nuclear absorption of negative pions from rest leads to the emission of nucleons and light nuclei. Although the details of the absorption process are still incompletely understood, two successive mechanisms are clearly discernible. First, the pion is absorbed on a nucleon cluster consisting of two or more nucleons. The constituents of this cluster share most of the energy and momentum of the incoming pion among each other. In the case of absorption on a two-nucleon cluster, this leads to the back to back emission of the nucleons with approximately equal energy ($\sim$70 MeV) as proposed by Brueckner et al.[1] In the case of absorption on a three- or four-nucleon cluster, strongly correlated neutron-deuteron and neutron-triton pairs as observed by Lee et al.[2] will result. The removal of the capturing cluster frequently leaves the residual nucleus in a highly excited state from which it decays first through particle emission (evaporation) and later through radiation. The particles emitted by this mechanism are generally of low energy and are emitted isotropically.

While inclusive neutron spectra have been measured to very low energies,[3-5] measurements of inclusive charged particle spectra below thresholds of 6, 8, and 9 MeV for protons, deuterons, and tritons respectively[6] had not been reported up to the time of this experiment, with the exception of an emulsion study by Fowler and Mayes.[7]

In the two previous papers[8,9] we have described the techniques that allow one to lower the energy threshold for the measurement of charged particle spectra substantially (to $\sim$1 MeV), and have reported the results obtained by this method in a study of pion induced α emission from ^{12}C.

In this paper we report a measurement of in-clusive p-, d-, and α-particle spectra from carbon, calcium, indium, and bismuth using the same techniques.

II. EXPERIMENTAL DETAILS

Figure 1 shows a schematic drawing of our experimental arrangement. Apart from the three NaI(Tl) crystals it is identical to the one used in our previous experiment.[8]

After initial moderation by 10 cm of polyethylene, the 100 MeV π^- beam of the synchrocyclotron of the Space Radiation Effects Laboratory at Newport News, Va., was monitored by the scintillation counters SC1 and SC2. Following further moderation and collimation to a semielliptical shape, the beam entered the 30 cm diameter vacuum chamber and was monitored in the thin plastic counter SC3, the normal of which formed an angle of $33°$ with the beam axis. The anticounter SC4 detected particles which did not stop in SC3.

The calcium, indium, and bismuth targets were installed parallel to SC3 at 2–3 millimeters distance from the beam exit face of the counter. They could be moved in and out of the beam to allow rate comparisons with and without target.

The particles emitted from SC3 and the target were viewed by 3 silicon surface barrier detectors which had an active area of 400 mm^2 each and were 0.5, 0.5, and 1.0 mm thick, respectively. They were installed at a distance of 61.4 ± 0.1 cm from SC3 in a plane parallel to that of the scintillator. This position in connection with the semielliptical shape of the beam entrance window of the vacuum chamber did not allow the detectors to directly view any part of the window. Each silicon detector was immediately followed by a 0.025 mm thick aluminum foil used as vacuum window, and a 2.54 cm thick NaI(Tl) crystal of 3.2 cm in diameter.
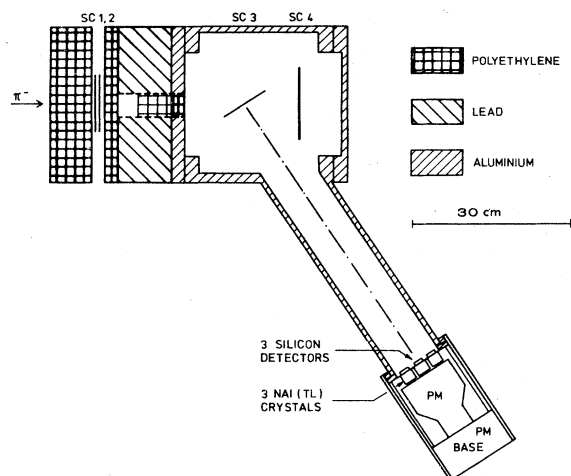
FIG. 1. Schematic of the apparatus.

All three crystals were coupled to the same photo-tube.

Depending on whether or not the charged particles stopped in the silicon detectors, they were identified either by their energy and time of flight (TOF) or by their energy loss in a silicon detector and the residual energy deposited in the NaI(Tl) crystal.. The minimum energies that the different fragments needed to penetrate the silicon detectors are given in Table I.

Owing to the finite resolution of the apparatus and the aluminum foils between the silicon detectors and the NaI(Tl) crystals particle identification was not possible in the vicinity of these energies.

Table II shows the thicknesses of the targets used in the experiment. As pilot B scintillator consists of 91.4% carbon and 8.6% hydrogen, and as the absorption on hydrogen is negligible, the plastic may be considered a pure carbon target for the purpose of this experiment. Therefore, it will henceforth be referred to as "carbon."

For each individual event, the time of flight, the energy deposited in the silicon detector, and

TABLE I. Minimum energies needed to penetrate the silicon detectors (MeV). Below these energies the particles were identified by their energy and time of flight, above by their residual energy and their energy loss in a silicon detector.

	Det. 1	Det. 2	Det. 3
Protons	8.2	8.2	12.2
Deuterons	10.9	10.9	16.3
α particles	32.6	32.6	48.6

TABLE II. Thicknesses of the targets.

Target	Thickness (cm)	Thickness (g/cm^2)
Carbon (SC3)	0.074	0.075
Calcium	0.10	0.16
Indium	0.035	0.26
Bismuth	0.031	0.31

the energy deposited in the NaI(Tl) crystal were written on magnetic tape. Frequent rate checks were made to verify the satisfactory performance of all components of the experiment.

The electronic threshold of the system was set equal to 0.5 MeV; particles depositing less energy in the silicon detectors were rejected. The detectors were calibrated using a ^{241}Am source. At one time the chamber was filled with ^{4}He and the mono-energetic (30.6 MeV) tritons from the reaction $\pi^- + {}^4\text{He} \rightarrow n + t$ were used to calibrate the NaI(Tl) crystals.

III. DATA ANALYSIS

A. Two-dimensional distributions

Using these calibrations, two-dimensional distributions of the total energy vs the time of flight and of the energy loss vs the total energy were plotted. In the ΔE vs E plane three bands corresponding to protons, deuterons, and tritons were clearly discernible and the particles were separated by inspection. In the E vs TOF distribution bands belonging to mass numbers 1, 2, 3, and 4 could easily be distinguished. As the E vs TOF identification does not allow the separation of isobars, events in the band corresponding to mass number 3 represented tritons and ^{3}He below the energy that tritons need to penetrate the silicon detector.

The corresponding distribution of events from the bismuth target looked quite different. The particle bands appeared weak, suggesting low production rates. In addition, a large background was present between 10 and 25 nsec TOF. As the silicon detectors were not sensitive to γ rays or electrons, we concluded that the background was caused by neutrons, and a quantitative analysis indeed shows it to be consistent with typical neutron multiplicities following pion capture in heavy nuclei.

Particle separation in the E vs TOF distributions was achieved either by inspection or by fitting a function composed of several Gaussians and an exponentially decaying background to cuts of 1 MeV width.

B. Measured spectra

Figure 2 shows the measured spectra of protons, deuterons, and α particles from the various targets. To augment the readability of the drawing, the spectra were regrouped into larger energy bins. As the solid angle acceptance was determined by the silicon detectors for both types of identificaton, no relative normalization of the two parts of the measured spectra was necessary.

C. Pion stops

The pion stopping rate for each target was determined from rate measurements with and without that target following SC3 in the beam. It was found that the ratio $1 \cdot 2 \cdot 3 \cdot \overline{4}/1 \cdot 2$ was within narrow limits proportional to the effective mass of the target (mass covered by SC3), multiplied by the specific energy loss of the incoming pions in the target. A correction, typically a few percent, was applied to account for the probability that a charged particle produced in either SC3 or the target hit the anticounter SC4.

D. Target absorption correction

When dealing with particles, the range of which is not large compared to the target thickness, one must distinguish between the spectrum "as measured" and the spectrum "as produced." As we have shown elsehwere,[8,9] a unique relationship exists between those two spectra, which enables one to derive the latter from the former. We have used the procedures described in Refs. 8 and 9 to unfold the measured spectra. For protons and deuterons Eq. (1) gives the production spectrum in terms of the measured spectrum $\nu(E)$, its derivative $\nu'(E)$, and the first and second derivative of the range-energy relation of the respective par-

ticle in the target material,

$$P(E) = P(G) \cdot G'(E)$$
$$+ t \left(\frac{\nu(E)R''(E)}{[R'(E)]^2} - \frac{\nu'(E)}{R'(E)} \right) \tag{1}$$

with $G = E[R(E) + t]$, where $E(R)$ is the inverse of the range-energy relation and t is the target thickness. For α particles all targets could be considered infinitely thick, i.e., particles produced with the highest energies could not or just barely penetrate the target. In this case Eq. (1) simplifies to

$$P(E) = t \cdot \left(\frac{\nu(E)R''(E)}{[R'(E)]^2} - \frac{\nu'(E)}{R'(E)} \right). \tag{2}$$

As Eq. (1) is a recursion formula, the unfolding has to proceed from high energies to low energies. As a consequence, any error made in the computation of the production spectrum at the highest energy will propagate through the calculation to the lower energies.

For the numerical calculations, the measured spectrum was fitted to an analytic function of the form

$$\nu(E) = \exp\left(a_0 + \sum_{i=1}^{n} a_i E^{b_i}\right) \tag{3}$$

with a_0, a_i, and b_i determined from a least squares fit. The strong dependence of $P(E)$ on both $\nu(E)$ and $\nu'(E)$ caused us to adopt the following precautions: We required the fit not to oscillate anywhere up to 6 MeV above the highest measured energy. In addition we obtained the derivative $\nu'(E)$ not by differentiating the fitted function $\nu(E)$ but by differentiating a polynomial of low order fitted to a few points in the immediate vicinity of E.

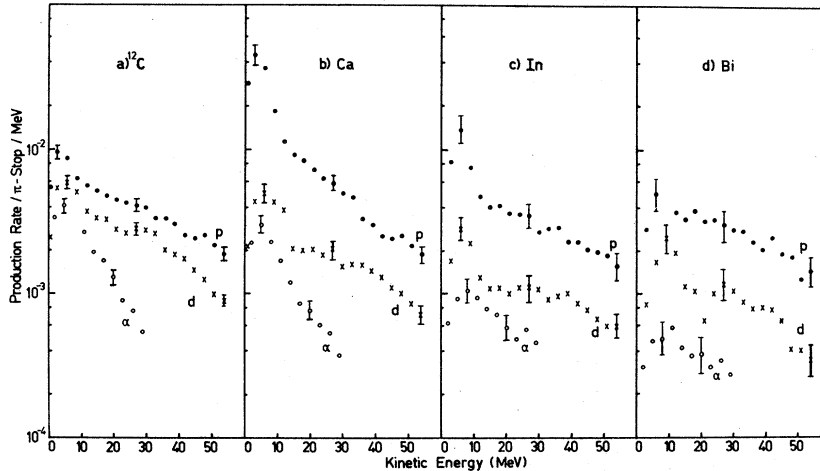This produced some differences from the results

FIG. 2. Measured particle production rates.

obtained in Ref. 8, when reprocessing the measured spectrum of α particles presented there, (see Table VII).

As was shown in Ref. 9, published range tables tend to be unreliable below energies of a few MeV. Therefore, the range-energy relation for the carbon target was measured using the method of homogeneous doping.[9] These results will be published elsehwere.[10]

IV. RESULTS

Figure 3 shows the unfolded spectra of protons, deuterons, and α particles emitted from carbon, calcium, indium, and bismuth following π^- capture from rest.

All unfolded spectra reach a maximum at energies of a few MeV. Whereas the proton spectra monotonically decrease above these energies, the deuteron spectra show a broad distribution centered around 30–35 MeV with a strong enhancement at low energies due to evaporation. The α-spectra decay nearly exponentially and appear to originate from evaporation only. These results are in agreement with recent measurements at SIN.[11] At energies below that of maximum production all spectra fall off very steeply. The energies at which the unfolded spectra go to zero depend strongly on the quality of the fits to the measured spectra and errors up to 2 MeV are

TABLE III. Low-energy limits of the unfolded particle spectra (MeV).

Target	Protons	Deuterons	α particles
Carbon	1.4	1.6	1.3
Calcium	1.4	2.0	1.7
Indium	4.2	4.7	4.5
Bismuth	4.2	6.5	4.1

possible. We nevertheless give these energies in Table III because the integrated production rates given in Table IV depend on them—although weakly—and because we believe the trends indicated in Table III to be real.

The production rates of protons, deuterons, and α particles integrated from the energies given in Table III to 55 MeV for protons and deuterons, and 30 MeV for α particles, are listed in Table IV; the average kinetic energies calculated over the same energy intervals are shown in Table V.

The energy-integrated production rate for protons reaches a maximum for calcium and then quickly decreases, in agreement with previous results.[6,12] The shape of the spectrum and the low average kinetic energy of protons produced from calcium indicate that a large fraction of the protons results from evaporation. The outstandingly large number of protons emitted by calcium was already noted by Castleberry et al.,[6] who observed protons above a threshold of 6 MeV. Castleberry's
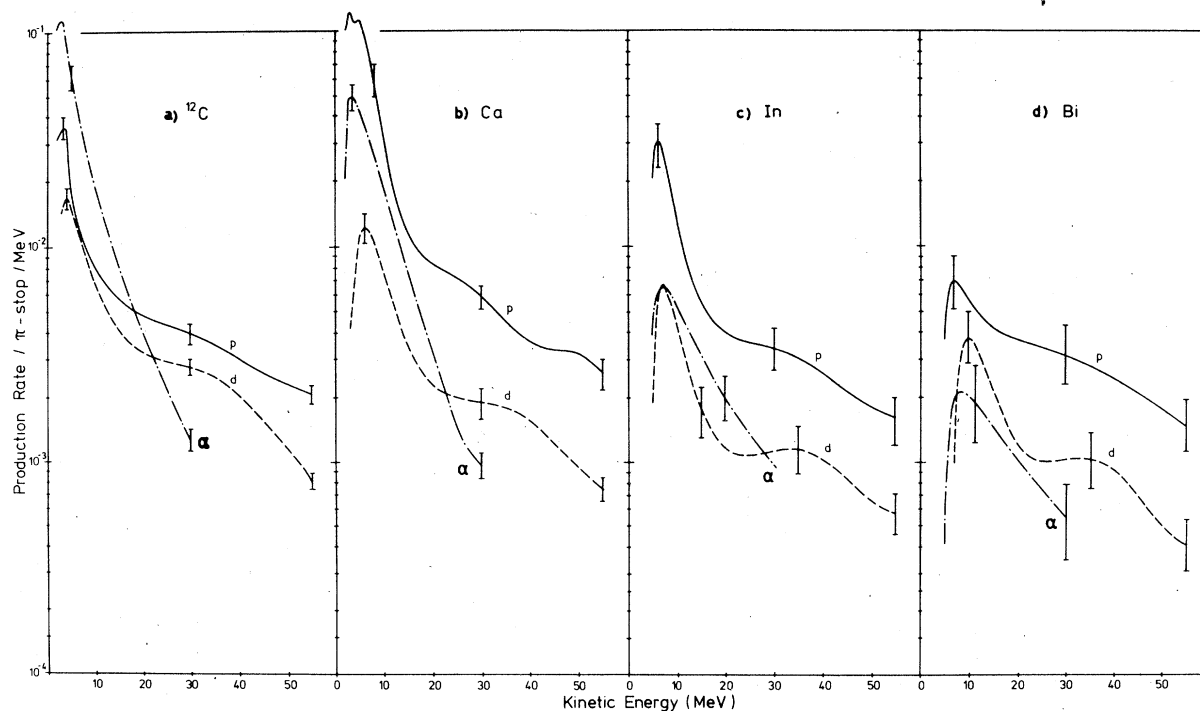

FIG. 3. Particle production rates, corrected for energy loss in the target.

TABLE IV. Energy-integrated production rates (%/stopped pion).

Target	Protons	Deuterons	α particles
Carbon	33.4 ± 3.5	21.4 ± 2.2	62.8 ± 6.3
Calcium	102.0 ± 15.1	16.3 ± 2.8	38.3 ± 5.8
Indium	28.5 ± 7.1	8.2 ± 2.0	7.6 ± 1.9
Bismuth	6.7 ± 5.2	6.2 ± 2.1	3.2 ± 1.5

TABLE VI. Particle production rates (%/stopped pion).

		Protons	Deuterons
Carbon	This work	22 ± 2.2	14 ± 1.5
	Castleberry	29 ± 5.8	21 ± 1.3
Calcium	This work	52 ± 7.4	11 ± 1.5
	Castleberry	46 ± 5.0	11 ± 1.3

observations on aluminum and sulfur suggest that this anomalous rate may not be due to a simple Z dependence. One of us (K.O.H.Z.) is planning to further investigate this problem. The energy-integrated production rate for deuterons monotonically decreases with increasing mass number of the target. The evaporation contribution is strongly suppressed for indium and bismuth.

Of particular difficulty in the analysis was the determination of the errors of the unfolded spectra and the integrated production rates. It did not seem feasible to us to trace the uncertainties— mostly statistical—of the measured spectra through the computations of the unfolding procedure. Therefore, an estimate of the errors of the unfolded spectra was obtained by unfolding each measured spectrum three times, once fitting through the measured counts, once through the upper limits of the error bars, and once through the lower limits. We are, however, aware that this approach cannot replace an exact calculation. Additional errors arise from the determination of the number of stopped pions, and—in the case of the proton and deuteron spectra from the calcium, indium, and bismuth targets—from the uncertainties in the subtraction of the contributions of SC3 to the measured spectra.

Because of the aforementioned difficulties, the errors quoted for the unfolded spectra and the integrated production rates contain as a further contribution the author's—naturally subjective— estimate of the quality of the measured spectra. Systematic uncertainties arising for example from inaccuracies of the used range-energy relations are not reflected.

V. COMPARISON WITH PREVIOUS RESULTS

In order to compare our results with those of Castleberry et al.,[6] the production rates of protons and deuterons from carbon and calcium were integrated between 6.1 and 55 MeV, and between 7.0 and 55 MeV, respectively. The numbers, together with the ones from Ref. 6, are listed in Table VI.

Whereas our values for carbon are somewhat lower than Castleberry's, agreement is good in the case of calcium.

Using the improved unfolding procedure and the newly measured range-energy relation for the carbon target, the measured spectrum of α particles presented in Ref. 8 was reanalyzed. Agreement with the production rates obtained in this experiment is excellent, except at energies below 2 MeV, where small differences occur (Table VII). These numbers are well confirmed by recent data taken at SIN.[13]

In Figs. 4(a) and 4(b) the α-cluster calculations by Kolybasov[14] are compared with our production spectra for protons and deuterons from carbon (normalized in one point). Keeping in mind that these calculations do not include evaporation, the agreement of the deuteron production rates is good. On the other hand, Kolybasov's calculations underestimate the number of high-energy protons, suggesting that the predominant mechanism for proton production is the absorption by a pair of nucleons.

Intranuclear-cascade-Evaporation calculations by Guthrie et al.[15] differ from our production spectra of protons and α particles from carbon [Figs. 4(a) and 4(c)].

TABLE V. Average kinetic energies (MeV).

Target	Protons	Deuterons	α particles
Carbon	16.8	17.3	6.6
Calcium	10.8	17.6	8.0
Indium	17.9	20.7	13.5
Bismuth	24.2	23.3	15.0

TABLE VII. Production rates of α particles from carbon (%/stopped pion).

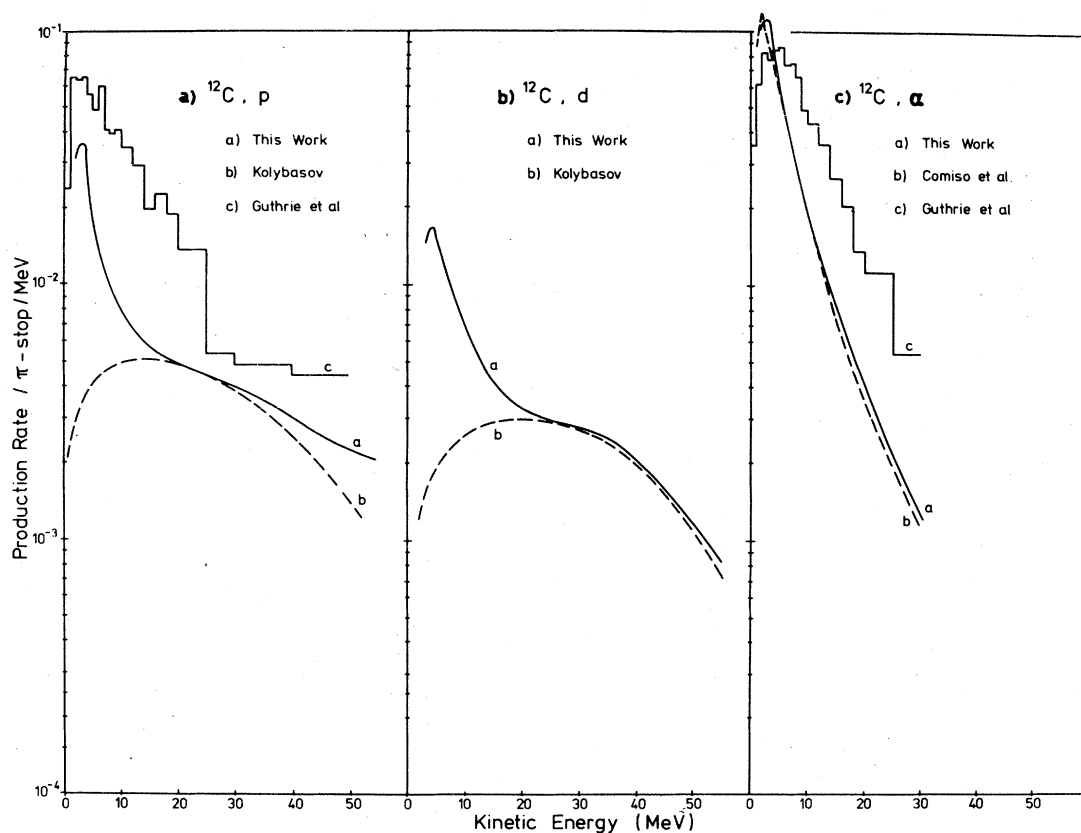| This work	Comiso et al.	Integration range (MeV)
60 ± 6.1	63 ± 5.3	1.5—30
52 ± 5.3	51 ± 4.2	2.5—30

FIG. 4. Comparison of particle production rates with α-cluster calculations by Kolybasov (Ref. 14) and intranuclear-cascade-evaporation calculations by Guthrie *et al*. (Ref. 15).

VI. CONCLUSIONS

Our results are in quantitative agreement with the values quoted by Castleberry[6] and Comiso.[8] The proton and deuteron spectra include both direct and evaporation contributions with the latter strongly suppressed for high Z targets. The α-particle emission appears to originate from evaporation—or breakup—only. Whereas high-energy protons seem to be predominantly the result of absorption by a pair of nucleons, the shape of the high-energy part of the deuteron spectrum from ^{12}C is in close agreement with the α-cluster calculations by Kolybasov [Fig. 4(b)], yet substantial contributions from other mechanisms cannot be excluded. The results of intranuclear-cascade-evaporation cal-

culations[15] deviate from our spectra for protons and α particles emitted from ^{12}C.

*Present address: Physik-Institut, Universität Zürich, 8001 Zürich, Switzerland.
†Present address: Max-Planck-Institut für Physik und Astrophysik, Föhringer Ring 6, 8000 München, West Germany.
[1]K. A. Brueckner, R. Serber, and K. M. Watson, Phys.

Rev. 84, 258 (1952).
[2]D. M. Lee, R. C. Minehart, S. E. Sobottka, and K. O. H. Ziock, Nucl. Phys. A182, 129 (1972); D. M. Lee, R. C. Minehart, S. E. Sobottka, and K. O. H. Ziock, *ibid*. A197, 106 (1972).
[3]H. L. Anderson, E. P. Hincks, C. S. Johnson, C. Rey,

and A. M. Segor, Phys. Rev. 133, B392 (1964).

[4]G. Campos Venuti, G. Fronterotta, and G. Matthiae, Nouvo Cimento 34, 1446 (1964).

[5]W. Dey, R. Engfer, H. Guyer, R. Hartmann, E. A. Hermes, H. P. Isaak, J. Morgenstern, H. Müller, H. S. Pruys, W. Reichart, and H. K. Walter, Helv. Phys. Acta 49, 778 (1976); R. Hartmann, H. P. Isaak, R. Engfer, E. A. Hermes, H. S. Pruys, W. Dey, H. J. Pfeiffer, U. Sennhauser, and H. K. Walter (unpublished); R. Hartmann, thesis, University of Zürich, 1978 (unpublished).

[6]P. J. Castleberry, L. Coulson, R. C. Minehart, and K. O. H. Ziock, Phys. Lett. 34B, 57 (1971): P. J. Castleberry, Ph.D. thesis, University of Virginia, 1970 (unpublished).

[7]P. M. Fowler and V. M. Mayes, Proc. Phys. Soc. London 92, 377 (1967).

[8]J. C. Comiso, T. Meyer, F. Schlepütz, and K. O. H. Ziock, Phys. Rev. Lett. 35, 13 (1975).

[9]J. C. Comiso, F. Schlepütz, and K. O. H. Ziock, Nucl. Instrum. Methods 133, 121 (1976).

[10]J. C. Comiso, F. Schlepütz, and K. O. H. Ziock (unpublished).

[11]H. K. Walter, *Proceedings of the 7th International Conference on High Energy Physics and Nuclear Structure, Zürich, 1977*, (Birkhäuser, Basel, 1977); H. S. Pruys, R. Engfer, R. Hartmann, E. A. Hermes, H. P. Isaak, H. J. Pfeiffer, U. Sennhauser, and H. K. Walter, Conference on Nuclear Reaction Mechanisms, Varenna, Italy, 1977 (unpublished).

[12]Y. G. Budyashov, V. G. Zinov, A. D. Konin, N. V. Rabin, and A. M. Chatrchyan, Zh. Eksp. Teor. Fiz. 62, 21 (1972) [Sov. Phys.—JETP 35, 13 (1972)].

[13]G. Mechtersheimer, G. Büche, U. Klein, W. Kluge, H. Matthaey, D. Münchmeyer, and A. Moline, Phys. Lett. B73, 115 (1978).

[14]V. M. Kolybasov, Yad. Fiz. 3, 729 (1966) [Sov. J. Nucl. Phys. 3, 535 (1966)].

[15]M. P. Guthrie, R. G. Alsmiller, and H. W. Bertini, Nucl. Instrum. Methods 66, 29 (1968).